# An In-Depth Study of Redox-Induced Conformational Changes in Charge Transport Characteristics of a Ferrocene-Alkanethiolate Molecular Electronic Junction: Temperature-Dependent Transition Voltage Spectroscopy Analysis

Hyunhak Jeong, Yeonsik Jang, Dongku Kim, Wang-Taek Hwang, Jun-Woo Kim, and Takhee Lee*

Department of Physics and Astronomy, and Institute of Applied Physics, Seoul National University, Seoul 08826, South Korea

ABSTRACT: We studied the temperature-dependent electrical properties of ferrocene-alkanethiolate molecular electronic junctions fabricated by a conventional solid-state device technique using a conducting polymer poly(3,4-ethylenedioxythiophene) stabilized with a poly(4-styrenesulfonic acid) (known as PEDOT:PSS) interlayer. We had previously observed unusual temperature-dependent electrical characteristics at a voltage polarity larger than +0.6 V and at temperatures higher than ~220 K (see *Adv. Funct. Mater.* **2014**, *24*, 2472). The origin of this distinctive behavior was ascribed to redox-induced conformational changes of the ferrocene-alkanethiolate molecules. We performed temperature-dependent transition voltage spectroscopy analysis based on the multibarrier tunneling model to support the proposed redox-induced conformational changes observed in the ferrocene-alkanethiolate molecular junctions. The obtained results were consistent with the unusual thermal characteristics of the ferrocene-alkanethiolate molecular junctions predicted by the proposed redox-induced conformational changes of the molecules.
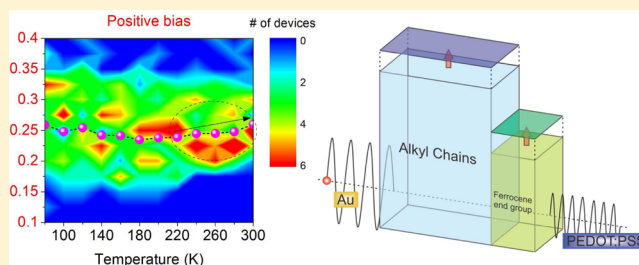
1. INTRODUCTION

The ultimate aim of molecular electronics is to overcome the limit of the conventional silicon-based solid-state electronics by utilizing either single molecules or a bundle of molecules as an active electronic device component. Since the first conceptual molecular diode theoretically proposed by Aviram and Ratner in 1974, the research field of molecular electronics has been widened and deepened by many research groups.[1−8] Although many issues must still be resolved to enable practical applications of molecular electronics, a large amount of comprehensive studies of the fundamental transport characteristics of molecular junctions and also of a wide range of potential device applications such as those for diodes, memory, transistors, and switches have been performed by these groups.[9−13] Recently, in an attempt to develop a reliable electronic device component, molecular diodes have gained increasing attention from researchers. Molecular diodes can be applied even in a single molecule junction by adopting various approaches that are able to engineer molecular junction parameters such as the molecular structure, electrodes, and their electronic coupling characteristics.[12,14−19] For example, Nijhuis et al. recently reported a robust molecular diode using ferrocene-alkanethiolate self-assembled monolayers (SAMs) and eutectic Ga and In (EGaIn) electrodes.[12,16,20] They demonstrated a large rectification ratio of up to ~1000 and reported that the strong asymmetric electrical characteristics could be interpreted by hopping assisted tunneling transport arising from the ferrocene-alkanethiolates and the electrodes.

Similar to these studies, we have also examined the possibility of the electronic device application by fabricating a large number of molecular devices based on ferrocene-alkanethiolate (denoted as FcC in this manuscript) SAMs using a conventional solid-state device fabrication technique both on rigid and flexible substrates.[21] In this previous study, we could only obtain a relatively small rectification ratio (~1.6) mainly due to the improper choice of the electrodes. Nevertheless, we observed a distinctive temperature dependence on the electrical characteristics; that is, the current density decreased as the temperature increased in a certain temperature range when a sufficient voltage was applied with a certain voltage polarity (i.e., when a large enough positive voltage was applied to ferrocene group side of the FcC molecular junction). This behavior was in contrast to the usually expected thermally activated charge transport in the molecular device junction or other device junctions in which, most times, the current density increases as the temperature increases. In that study,[21] we suggested the unusual thermal characteristics are probably due to the redox-induced conformational changes of the ferrocene-alkanethiolates in the molecular junctions. While the analysis was quite reasonable and consistent with the experimental results, further evidence was needed to support our suggested explanation.
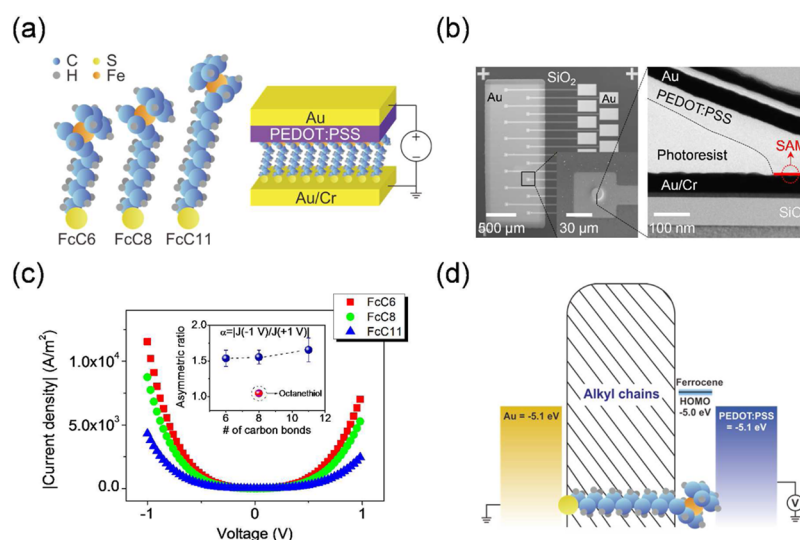
Figure 1. (a) Schematic illustrations of molecules and molecular junction structure in this study. (b) Scanning electron microscope and cross-sectional transmission electron microscope images of the molecular devices. (c) Representative electrical characteristics of the FcC molecular devices. We characterized ∼50 devices for each molecule. The inset shows the asymmetric ratio (see the main text for the definition) of our molecular junctions. The asymmetric ratio of a control junction using octanethiol was also depicted in the plot. (d) Suggested energy band diagram of our molecular junction in equilibrium state.

Here, we report the temperature-dependent electrical characteristics of the FcC molecular junctions fabricated by a conventional solid-state device technique using a PEDOT:PSS (poly(3,4-ethylenedioxythiophene) stabilized with a poly(4-styrenesulfonic acid)) interlayer. We have observed unusual temperature-dependent electrical characteristics at voltage polarities larger than +0.6 V and at temperatures higher than ∼220 K. The origin of this distinctive behavior was ascribed to redox-induced conformational changes of the ferrocene-alkanethiolate molecules. The analysis of the results of the temperature-dependent transition voltage spectroscopy (TVS) based on a multibarrier tunneling model supports the occurrence of the proposed redox-induced conformational changes in the ferrocene-alkanethiolate molecular junctions.

2. EXPERIMENTAL SECTION

2.1. Device Fabrication. To fabricate the molecular junctions, we followed the fabrication process reported in our previous work.[21,22] Here, the main features of the fabrication procedures are described again as follows: first, square-shaped SiO$_2$ (100 nm thick)/Si substrates with dimensions of 1.5 × 1.5 cm^2 were prepared in a general cleaning process using acetone, methanol, 2-propanol, and deionized water by immersing the substrates into each solution with ultrasonication for 5 min. The patterned bottom electrodes (Au; 50 nm thick/Cr; 10 nm thick) were then generated using photolithography and metal evaporation by spin-coating a photoresist (Az5214E, purchased from Az Electronic Materials, Darmstadt, Germany) on the substrates at 4000 rpm for 1 min and then fabricating the bottom electrode patterns following conventional photo-lithography procedures (416 nm wavelength, intensity of 20 mW/cm^2 for 10 s). Next, the metal film consisting of 50 nm of Au and 10 nm of Cr was deposited on the substrates using an e-beam evaporator with a rate of ∼0.1 Å/s at a pressure of ∼10^{-6} Torr to obtain a smooth, molecular layer on the bottom electrode. The isolation layer that specifies the contact surface on the bottom electrodes on which the molecular layer is deposited was then generated by a photolithography process

using the Az5214E photoresist. Following the formation of the isolation layer, the sample was hard-baked at 190 °C for ∼2 h to prevent the isolation layer from dissolving in the SAM solution. The samples were then dipped into dilute solutions of anhydrous ethanol that contain ferrocene-alkanethiolate molecules at a concentration of ∼3 mM for 1−2 days in a N$_2$-filled glovebox. The molecules used in this study are shown on the left-hand side of Figure 1a and are 6-ferrocenyl-1-hexanethiol (denoted as FcC6), 8-ferrocenyl-1-octanethiol (FcC8), and 11-ferrocenyl-1-undecanethiol (FcC11). These molecules are commercially available and were purchased from Sigma-Aldrich Co. and Dojindo Molecular Technologies, Inc. Following the SAM formation on the revealed bottom electrode surface, we softly rinsed the substrates using anhydrous ethanol for ∼10 s to remove the unbonded molecules on the electrode surface. The substrates were then dried in the glovebox for ∼2 h prior to an interlayer deposition. Here, we used a conducting PEDOT:PSS polymer as the interlayer to prevent direct metal filament formation during the evaporation of the top electrode metal, which results in electrically short circuit junctions and eventually a low device yield.[23,24] The PEDOT:PSS (PH1000 purchased from Clevios and doped with dimethyl sulfoxide and Triton X-100 for a higher conductivity[25]) was spin-coated on the substrates at 3500 rpm for 30 s and dried for ∼2 h in the glovebox. After coating, we evaporated the top electrode metal (Au; 50 nm thick) on the substrate using a shadow mask and e-beam evaporator. Finally, to remove the direct conduction pathway from the bottom electrodes to the top electrodes through the PEDOT:PSS layer, we used O$_2$ gas (11 sccm, 60 mTorr, 50 W forward power) in a reactive ion etching process to etch the residual PEDOT:PSS layer that was not covered by the top Au electrode. A schematic illustration of the fabricated junction structure is displayed on the right-hand side of Figure 1a. Additionally, Figure 1b shows the scanning electron microscope and cross-sectional transmission electron micro-scope images of our molecular junctions.

2.2. Electrical Characterization. The electrical character-istics of the FcC molecular junctions were measured using a
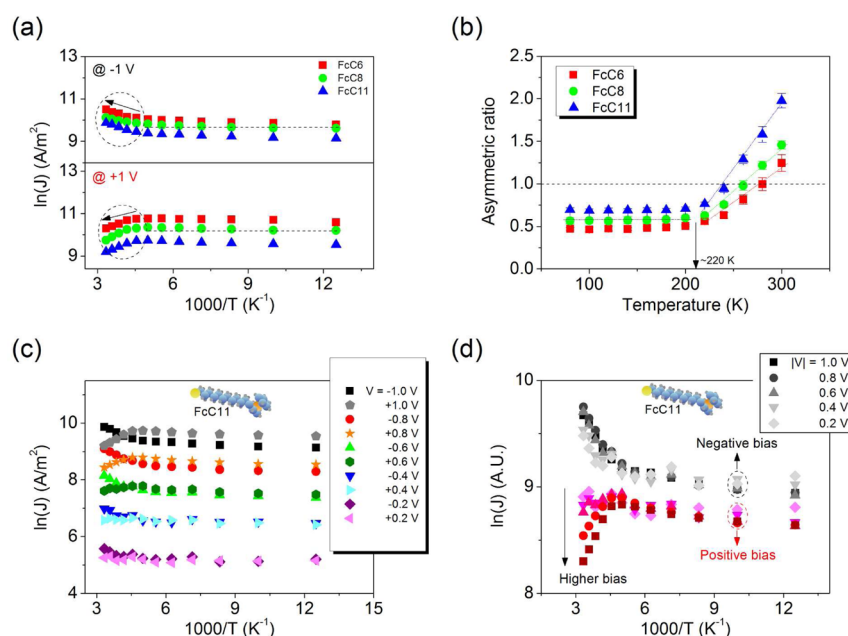
Figure 2. (a) Arrhenius plots of representative FcC molecular devices at ±1 V. (b) Variation of the asymmetric ratio versus temperature from 80 to 300 K for each representative FcC molecular device. (c) Arrhenius plots for an FcC11 molecular device under different applied voltages from ±0.2 to ±1.0 V with a ±0.2 V interval at each voltage polarity. (d) Normalized Arrhenius plots of an FcC11 molecular device at each voltage (from c).

temperature variable probe station system (ST-500 purchased from Janis Research Company, Inc.) and a semiconductor parameter analyzer (Keithley 4200SCS). We applied the voltage to the top electrodes while the bottom electrodes were grounded as shown in Figure 1a. The voltage was swept from −1 to +1 V. For temperature variable characterizations, we used liquid nitrogen and a feedback looped heat generator to adjust the samples' temperature. The temperature was varied from 80 to 300 K at intervals of 20 K. Additionally, the measurements at the low temperatures were performed by raising the temperature and vice versa. The obtained results were consistent with each other.

3. RESULTS AND DISCUSSION

3.1. Electrical Characteristics of FcC Molecular Devices Revisited: Temperature-Dependent Analysis. As mentioned above, in this study, we used three ferrocene-alkanethiolate molecules of different lengths that have a different number of alkyl chains (CH_2) with a single ferrocene end group as shown in Figure 1a. The molecules have 6, 8, or 11 alkyl chains. In the absence of the ferrocene end group, the molecules are merely alkanemonothiols. The main transport mechanism through the alkanemonothiol molecules is known to be direct tunneling due to the saturated σ orbital structures and a large gap between the highest occupied molecular orbital (HOMO) and the lowest unoccupied molecular orbital (LUMO) (i.e., large barrier height).[5] Therefore, the current−voltage (I−V) characteristics show a symmetric behavior at both voltage polarities due to the symmetrical molecular structure in conjunction with the large barrier height.[26,27] However, when the ferrocene end group is attached to the end of the molecule, the devices exhibit asymmetric I−V characteristics because the HOMO of the ferrocene end group lies near the edge of the Fermi level of the top electrode metal, similar to Au.[12,16,20,21] In this case, HOMO (of ferrocene) mediated tunneling (i.e., hopping mediated tunneling) occurs only at the forward bias, resulting in an increase in the tunneling current

due to the reduction in the effective barrier width.[12,16] For example, Nijhuis et al. has reported a high rectification ratio value (up to ~1000) in EGaIn-based molecular junctions employing ferrocene-alkanethiolates.[20] Figure 1c shows the representative I−V characteristics of our FcC molecular junctions with the PEDOT:PSS interlayer. To plot the data, we log-averaged the data from working FcC molecular devices; these values were determined by following the previously reported criteria without any particular data selection.[28] Here, ~ 50 molecular devices for each molecule length were analyzed, and the device yield was found to be ~50%. For easy comparison, absolute values of the current densities are shown in Figure 1c. The inset depicts a statistically derived asymmetric ratio (α), defined as $\alpha = | J(-1\ V)/J(+1\ V) |$, where $J(\pm1\ V)$ represents the current densities at +1 V and −1 V, respectively. We found that our molecular devices also showed asymmetric electrical characteristics; the devices showed higher current densities at negative voltages (forward bias, see Figure 1a for voltage connection), and the representative α was consistently found to be ~1.6 in agreement with previous observations.[21] This value is lower than that of other reports because of the different junction structures especially for the top electrode material.[12,16,20] In addition to the nature of the top electrode material, the flatness of the bottom electrode and the concentration of impurities in the ferrocene-alkanethiolate solution may also influence the asymmetric ratio.[29,30] However, the assignment of the asymmetric behavior to the presence of the ferrocene moiety was correct because a control experiment using octanethiol (HS-($CH_2)_7$-CH_3) molecular junctions without ferrocene moieties showed a value of α close to unity, as shown in the inset of Figure 1c. Figure 1d shows a suggested energy band diagram of our molecular junction in the equilibrium state. The energy state values presented in the figure were either measured using the Kelvin probe technique or taken from the literature.[12,16,21] On the basis of the energy band diagram analysis, we could understand the origin of the low asymmetric ratio found in our molecular junction structure,

which is unlike the case of molecular junctions that employ EGaIn as the top electrode. Assuming a potential drop across the ferrocene moiety and the PEDOT:PSS layer of 0.3 V under an applied bias of ±1 V,[16] the HOMO of the ferrocene moiety lies between the bias window of the top and bottom electrodes for both voltage polarities. Therefore, in both voltage polarity regimes (forward and reverse biases), the HOMO contributes to the tunneling transport, resulting in similar current densities at each voltage polarity and a low asymmetric ratio. Nevertheless, due to the more accessible energy state of the ferrocene HOMO from the top electrode under the forward bias (−1 V), our devices show slightly different current densities at each voltage polarity as well as the off unity asymmetric ratio. Therefore, to achieve a high asymmetric ratio, careful engineering of the contact properties between the ferrocene-alkanethiolates and the electrodes is crucial.

To elucidate the charge transport characteristics of the FcC molecular junctions, we performed temperature-dependent current−voltage ($I-V-T$) characterizations. Figure 2a depicts Arrhenius plots ($\ln(J)$ versus $1000/T$) of each representative molecular junction at ±1 V. Here, we analyzed ~25 FcC molecular devices for each molecule length. The temperature was varied from 80 to 300 at 20 K intervals. As shown in Figure 2a, the current density characteristics exhibited almost temperature-independent behaviors regardless of the number of alkyl chains, implying that direct tunneling is the dominant charge transport mechanism. However, at high temperatures (≥~220 K), the current density values changed slightly with different trends for increasing temperatures at each voltage; i.e., the values at −1 V (forward bias) increased with increasing temperature while the values at +1 V (reverse bias) decreased with increasing temperature. As shown in Figure 2b, such different trends of the current density changes result in the variation of the asymmetric ratio with temperature starting at approximately 220 K. The asymmetric ratio decreased with decreasing temperature until ~220 K and then remained steady at below unity for the lower temperatures (i.e., $J(+1\ V) > J(−1\ V)$). At the negative voltage, the increased current densities can be explained by a contribution of a weak hopping conduction (i.e., hopping-assisted tunneling; note that, however, the dominant charge transport mechanism is tunneling as we mentioned above) via the ferrocene moiety HOMO to the top electrodes.[12,16] In molecular junctions, this kind of transition of charge transport mechanism is observable depending on various junction parameters such as number of molecular chain length,[31,32] temperature,[32−34] applied bias,[33,34] etc. Specifically, due to the dependence of energetic parameters (degree of thermal agitation/activation energy) of thermally activated charge transport (thermionic/hopping conduction), these transitions might be observed more easily when the transport characterizations are performed over a broad range of energy spectrum.

On the other hand, the decreasing current densities at the positive voltage are an unusual feature that are unexpected in the $I-V-T$ characterizations of molecular junctions.[35,36] To elucidate their characteristics in detail, we used the voltage-dependent Arrhenius plots of a representative FcC11 molecular device as shown in Figure 2c and 2d. Figure 2c shows the Arrhenius plots of the FcC11 molecular device under different applied voltages ranging from ±0.2 V to ±1.0 V with a ± 0.2 V interval at each voltage polarity. The analysis of the data confirms that the temperature dependence of the current densities at the negative bias can be interpreted by the weak

hopping conduction (along with the dominant charge transport mechanism of tunneling) and not thermionic emission.[21] For the positive voltage, the strength of the current density temperature dependence (i.e., the slopes of the plots over ~220 K) varied with the magnitude of the applied bias. In particular, the current densities began to drop more rapidly at the applied bias values higher than approximately +0.6 V. To clearly visualize this effect, we show the normalized Arrhenius plots of the device at each voltage in Figure 2d. Examination of the figure shows that the current density temperature dependence became stronger with increasing applied voltage at the positive voltage while it remained almost constant at the negative bias. The detailed explanation about this voltage dependence will be presented in the following paragraph. Consequently, the analysis of the unusual characteristics should consider not only the thermal effects but also the bias-dependent effects.

In our previous report, we presented two probable origins of this unexpected feature of our molecular junctions.[21] As mentioned above, these features could be closely related to the presence of ferrocene as the end group and their properties as the contacts with the PEDOT:PSS layer. Ferrocene moieties are well-known for their strong electron-donating properties and how they quite easily assume their oxidized form (ferrocenium cation).[37] This strong oxidizing property makes the ferrocene-alkanethiolates easily oxidized and reduced even under relatively small applied voltages.[38] Cyclic voltammetry experiments using the ferrocene-alkanethiolate SAMs identified this behavior by an oxidation peak of around +0.6 V with respect to the Au electrode.[39,40] When the ferrocene moiety is oxidized with applied voltages higher than +0.6 V, the electrostatic interaction between the ferrocenium cations and the bottom electrode produces a redox-induced conformational change of the SAMs.[39] This is because the positively charged (oxidized) ferrocenium cations at the end of ferrocene-alkanethiolate SAMs will exert a repulsive force on the bottom electrodes and laterally to each other. In this dynamic state, the ferrocene-alkanethiolate SAMs may reach their equilibrium state by the conformational changes through the two following mechanisms: (1) The SAMs are reoriented to be more perpendicular to the bottom Au electrodes, i.e., the tilt angle decreases.[39] This is schematically depicted in Figure 5a. When the molecules in the SAMs assume a more vertical configuration (i.e., tilt angle decreases), the effective distance between the ferrocenium cations increase, leading to an increase in the tunneling barrier width for through-space transport in the alkyl chains.[41,42] (2) The ferrocenium cations push each other outward. Regardless of the conformational change in the main body of the structure of the ferrocene-alkanethiolate (the alkyl chains), the oxidized ferrocene moieties exert a repulsive force on each other and bend randomly (disordering effect).[39,43] This is schematically depicted in Figure 5c. This effect leads to poor contact of the molecules with the PEDOT:PSS interlayer (the detailed explanation will be given in the following section). In either mechanism, the redox-induced conformational changes result in the decrease of the current densities at the positive voltages above +0.6 V. Additionally, because the conformational changes require sufficient thermal energy to rearrange the orientation of the SAMs, this effect becomes stronger when the temperature increases above 220 K. Also in such a manner, the voltage dependence of the degree of current density decrease in Figure 2d can be explained. The voltage dependence is closely related
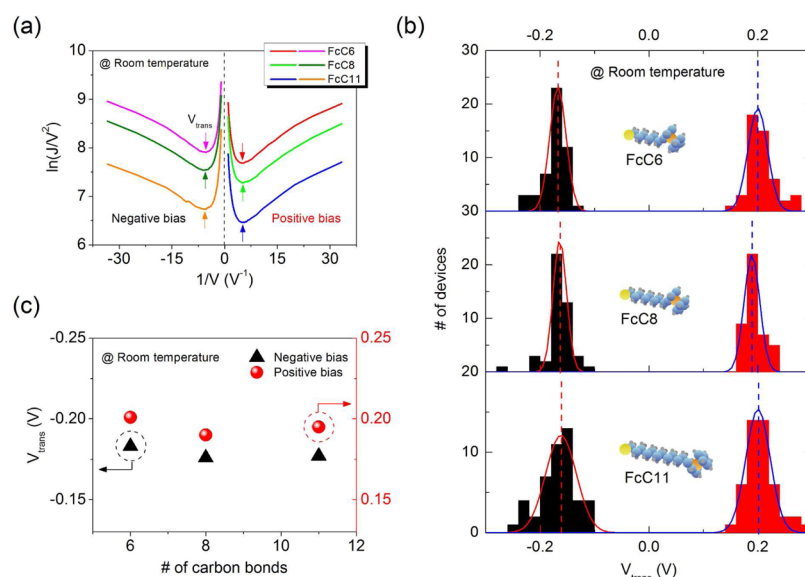
Figure 3. (a) Fowler–Nordheim plots of representative FcC molecular devices at room temperature (300 K) under each voltage polarity. Arrows depict inflection points of the plots that represent V_{trans} values. (b) Statistical histograms of the V_{trans} values of each representative molecular junction at both voltage polarities. Fitting curves using a normal distribution function are also depicted. (c) Averaged V_{trans} values at each voltage polarity.

to the degree of oxidation of the ferrocene moieties because the unusual temperature dependence of current density at positive bias was attributed to the oxidation process of the ferrocene moieties. As the oxidation process requires sufficient energy to occur,[39] for example electrostatic potential in our case, the degree of oxidation of the ferrocene moieties (i.e., the population of the ferrocenium cation) would increase as the magnitude of applied voltage increases, which will eventually result in a stronger temperature dependence of the unusual behavior. Note that here we were impossible to estimate how many ferrocene moieties would be oxidized at any given time. Meanwhile, the reduction process in the FcC molecular junction is also worthwhile to be discussed. Here, the electrical characteristics of our molecular junctions were measured using a probe station system and a semiconductor parameter analyzer. Specifically, we applied the voltage to the top electrodes while the bottom electrodes were grounded and the voltage was swept from −1 to +1 V. After the voltage sweep was completed, it changed immediately to 0 V. In such a case, the ferrocene moieties would be oxidized by the positive voltage over ∼0.6 V. Then, since the terminal group of the FcC monolayer is neutral in the reduced form,[39] the reduction reaction would occur when the applied voltage changes to 0 V by a charge relaxation process from the electron reservoir (i.e., the top electrodes) to the oxidized ferrocene moieties. On the basis of the discussion, we could expect that the redox-induced conformational change is a transient effect, not a permanent effect. This can be indirectly confirmed by the fact that the obtained results from the measurements at the low temperatures performed by raising the temperature and vice versa were consistent with each other. Also, we can expect that the orientation changes induced by the oxidized ferrocene moieties will disappear as the ferrocene moieties are reduced and the monolayer restores its original conformation as we depict in Figure 5a and 5c.

The above discussion is fairly reasonable; nevertheless, further careful studies are still needed to confirm the validity of the mechanisms. In the following section, we describe temperature-dependent transition voltage spectroscopy charac-

terizations performed in order to examine the validity of the proposed conformational change effects and to understand the temperature-dependent charge transport characteristics of our FcC molecular junctions in detail.

3.2. Temperature-Dependent Transition Voltage Spectroscopy Analysis of FcC Molecular Devices. In the field of molecular electronics, transition voltage spectroscopy (TVS) has been found to be a promising tool for understanding the charge transport mechanism through molecular junctions, especially for the tunneling transport involving frontier molecular orbitals and the Fermi level of the electrodes.[44−46] On the basis of the fact that the effective tunneling barrier shape can be modulated by the applied voltage on the sandwiched molecules between the electrodes, the examination of the Fowler–Nordheim plot (F–N plot; $\ln(J/V^2)$ versus $1/V$) can provide general insight into the energy offset between the frontier molecular orbital and the Fermi level of the electrodes.[44−46] The advantage of the TVS analysis is that, because it does not depend on a detailed microscopic model, it can be applied to various molecular systems to extract the energy level alignment.[47,48] Since Beebe et al. first proposed this technique to investigate the transport properties of molecular junctions, TVS has been widely adopted by many research groups and has been developed both theoretically and experimentally to consider the more subtle features of molecular junctions such as an asymmetric coupling effect.[49,50]

Here, we applied this technique to investigate our molecular junctions. As mentioned above, according to the temperature dependence analysis, tunneling transport is the dominant transport mechanism in our FcC molecular junctions. Although the weak hopping transport mediated by the HOMO of the ferrocene moiety also influenced the charge transport characteristics, this effect may be too weak to dominate the entire charge transport characteristics due to the large barrier height of the long alkyl chains. In this case, we could assume that the energy band diagram of our molecular junctions is represented by an effective single barrier model by considering the energetic contact between the ferrocene moieties and the PEDOT:PSS layer as an individual barrier. This idea is based on the
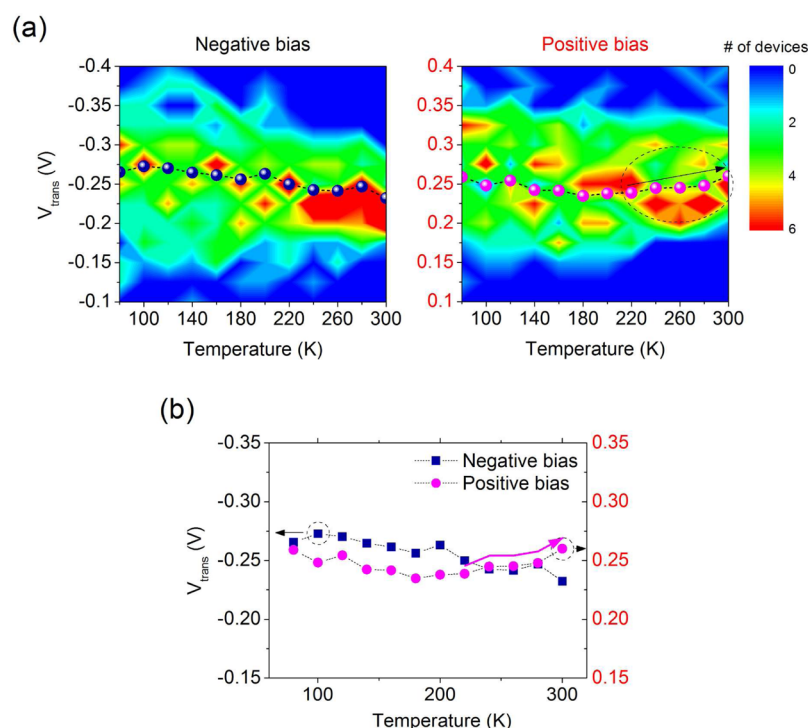
Figure 4. (a) Contour plots of statistical histograms of the V_{trans} values versus the temperatures at each voltage polarity. In the plots, the averaged values are depicted as data points and dotted lines. (b) Averaged V_{trans} values are redepicted for clear identification.

multibarrier tunneling (MBT) model, previously reported by our group.[51] The main concept of the MBT model is the generalization of the Simmons tunneling model by dividing a single rectangular tunneling barrier of the molecule into the set of individual barriers such as the molecular−chain body barrier and the metal−molecule contact barriers.[51] On the basis of this model, we could consider our FcC molecular junctions as an effective tunneling barrier replaced with a set of individual tunneling barriers: the alkyl chains and ferrocene moiety−PEDOT:PSS layer contact. Figure 3a presents the F−N plots of representative FcC molecular devices at room temperature (300 K) under each voltage polarity. In an F−N plot, the transition voltage (V_{trans}) is determined by the inflection point ($d(\ln(J/V^2)/d(1/V) = 0$) that eventually becomes the same as the minimum point of the plot. In Figure 3a, the minimum points of each plot that represent V_{trans} of each representative molecular device are marked. To extract the most probable V_{trans} values, we characterized the V_{trans} values of each set of ~50 FcC molecular devices. Figure 3b and 3c shows the statistical histograms and the obtained results for the V_{trans} values at room temperature. We plotted the fitting curves using a normal distribution function and their averages as dotted lines. On the basis of these histograms, it was statistically determined that the averaged V_{trans} values were −0.183 ± 0.021 V, −0.176 ± 0.025 V, and −0.177 ± 0.035 V for the FcC6, FcC8, and FcC11 devices, respectively, at the negative voltage polarity and 0.201 ± 0.032 V, 0.190 ± 0.030 V, and 0.195 ± 0.029 V at the positive voltage polarity. These results suggest three features: (1) the V_{trans} values at the positive voltage (i.e., the effective barrier height at the positive voltage) are larger than those at the negative voltage for each molecule, in agreement with the asymmetric I−V characteristics shown in Figure 1c (i.e., the current densities were higher at the negative voltage than at the positive voltage). This type of difference

between the V_{trans} values at each voltage polarity can be easily found in many molecular systems when the electronic coupling strength between the molecules and the electrodes differ at the two sides.[50−52] However, here, it should be noted that the V_{trans} values may not be identical to the effective barrier heights.[44,45,47,48] Therefore, we cannot compare the absolute barrier height magnitudes; we can compare only their differences. (2) The V_{trans} values show values that are much different than those of the molecular junctions using the usual alkanethiolates that do not contain the ferrocene end group (i.e., ~1.2 V for the Au/alkanethiolate-PEDOT:PSS/Au junction).[51,53] This indicates that the introduction of the ferrocene end-group does influence the charge transport characteristics. However, it should again be noted that this cannot be used for evaluation of how much the effective barrier height has been changed. (3) Regardless of the number of alkyl chains, the V_{trans} data showed similar values within the error range. This can be expected due to the fact that the dominant charge transport mechanism through the ferrocene-alkanethiolates is tunneling via the long alkyl chains and their HOMO−LUMO gap remains effectively constant as the number of alkyl chains changes.[26,54,55] These findings agreed well with the investigation of the basic transport characteristics at room temperature described in the previous section.

Furthermore, following this analysis, we investigated the temperature-dependent charge transport characteristics and especially the unexpected feature at the positive voltage. Figure 4a shows the contour plots of statistical histograms of the V_{trans} values versus the temperatures at each voltage polarity. Here, we characterized a total of ~25 working molecular devices and depicted their averaged values as data points and dotted lines in the plots. Examination of the statistical results shows that V_{trans} values remained almost constant as the temperature changed and showed similar values at both voltage polarities. However,
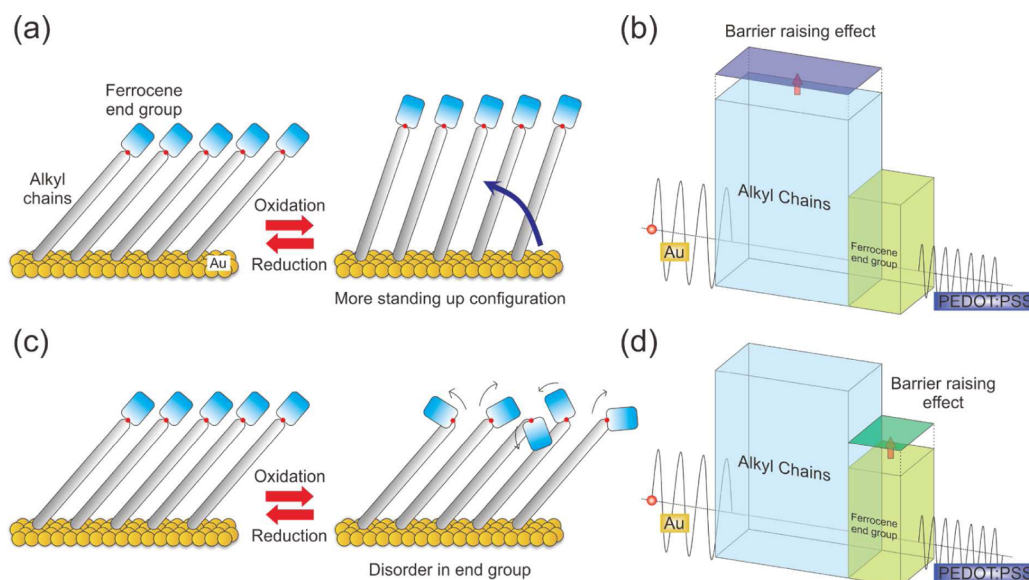
Figure 5. Schematic illustrations of proposed redox-induced conformational changes of the ferrocene-alkanethiolates and their corresponding barrier raising effect based on the MBT model. (a) More stand-up configuration of the alkyl chain body and (b) corresponding increase of the barrier height of the alkyl chain body. (c) Disorder in the ferrocene end-group and (d) corresponding increase of the barrier height of the ferrocene end-group.

at temperatures higher than ~220 K, they showed slightly different properties at each voltage, i.e., the V_{trans} values slightly increased at the positive voltage in contrast to the behavior at the negative voltage; this implies that the effective barrier height increased. To visualize this more clearly, we individually replotted the averaged V_{trans} values versus the temperatures, as shown in Figure 4b. Examination of the plot shows that the V_{trans} values at the positive voltage started to increase at temperatures higher than ~220 K, unlike the case at the negative voltage. This subtle distinction at the positive voltage can be explained consistently by the redox-induced conformational changes of the ferrocene-alkanethiolates, as mentioned above. In the molecular systems, the charge transport through the molecules can be strongly influenced by the molecular conformations, which may lead to the change of the transition voltage due to conformational changes.[56] Figure 5a and 5c shows schematic illustrations of two possible redox-induced conformational changes of the ferrocene-alkanethiolates at the positive voltage. When the ferrocene moieties are oxidized by the positively applied voltage, the SAMs are reoriented to be more perpendicular with the bottom Au electrodes, i.e., the tilt angle decreases as shown in Figure 5a.[39] As the molecular tilt angle decreases, the chain-to-chain tunneling (i.e., through-space tunneling) between the adjacent alkyl chains becomes less significant in addition to the already existing through-bond tunneling.[57,58] This results in the reduction of the strength of the field emission by the reduction of electric field, leading to a weakening of the electric field induced barrier lowering effect and thus appearing as a barrier raising effect.[58] In Figure 5b, this effect is schematically presented based on the MBT model. On the other hand, the coupling strength between the molecules and the electrodes on each side, i.e., the contact properties, can also influence the contact barrier height based on the MBT model.[51,59] Usually poor contact causes an increase in the contact barrier height due to poor charge transfer efficiency between the molecules and the electrodes.[51,59] For example, we previously reported that the difference in the specific bonding nature of alkanethiolates to the top electrodes (physical bond) could result in the increase of contact barrier height.[51] In this

report, the deduced contact barrier height of the poor physical contact (methyl-Au) has been found to be higher than that of the good chemical contact (thiol-Au). In our case, the repulsive force between each individual ferrocenium cation could weak the electron overlapping (hybridization) of neighboring ferrocenium molecular orbitals or atomic orbitals of the top metal electrodes because the valence electrons are missing. Therefore, this effect could reduce the molecular electron transfer rates between them, which can be considered as poor physisorbed contact. Therefore, we can expect that the disorder in the ferrocene end-group induced by the redox process of the ferrocene-alkanethiolates leads to poor physisorbed contact with the PEDOT:PSS layer, causing an increase in the contact barrier height. Figure 5d schematically presents this effect based on the MBT model. Here, we considered these two effects based on the MBT model, but both effects can lead to the increase in the total effective barrier height, which will consequently result in an increase of the V_{trans} values at a positive voltage. On the basis of this analysis, we can conclude that the unusual $I-V-T$ characteristics at positive voltages are supported by the redox-induced conformational changes of the ferrocene-alkanethiolates that are consistent with temperature-dependent TVS results. Nevertheless, we emphasize here that a more careful and direct verification of this type of conformational change must be obtained in order to strengthen our analysis and fully understand the nature of this effect in future studies.

4. CONCLUSIONS

In summary, we investigated the temperature-dependent electrical characteristics of the ferrocene-alkanethiolate molecular junctions using the PEDOT:PSS interlayer. We fabricated and analyzed a statistically sufficient number of devices to ensure the reliability of the data. In particular, we consistently observed unusual temperature-dependent electrical characteristics at a voltage polarity larger than +0.6 V and at temperatures higher than ~220 K. The origin of this distinctive behavior was attributed to the redox-induced conformational changes of the ferrocene-alkanethiolate molecules. We used the

transition voltage spectroscopy (TVS) analysis to understand the electrical characteristics of these molecular junctions. From the analysis, we found that the obtained TVS results were consistent and in good agreement with the measured electrical characteristics. Additionally, we performed a temperature-dependent TVS analysis based on the multibarrier tunneling model to support the proposed redox-induced conformational changes of the molecules. Our study suggests the significance of the consideration of the macroscopic structural organization of the molecular junction as well as the intrinsic molecular properties, which includes the redox processes or molecular conformations, to understand the charge transport characteristics of the molecular junctions.

■ AUTHOR INFORMATION

Corresponding Author
*E-mail: tlee@snu.ac.kr.

Notes
The authors declare no competing financial interests.

■ ACKNOWLEDGMENTS

■ REFERENCES

(1) Reed, M. A.; Zhou, C.; Muller, C. J.; Burgin, T. P.; Tour, J. M. Conductance of a Molecular Junction. *Science* **1997**, *278*, 252−254.

(2) Joachim, C.; Gimzewski, J. K.; Aviram, A. Electronics Using Hybrid-Molecular and Mono-Molecular Devices. *Nature* **2000**, *408*, 541−548.

(3) Nitzan, A.; Ratner, M. A. Electron Transport in Molecular Wire Junctions. *Science* **2003**, *300*, 1384−1389.

(4) McCreery, R. L. Molecular Electronic Junctions. *Chem. Mater.* **2004**, *16*, 4477−4496.

(5) Love, J. C.; Estroff, L. A.; Kriebel, J. K.; Nuzzo, R. G.; Whitesides, G. M. Self-Assembled Monolayers of Thiolates on Metals as a Form of Nanotechnology. *Chem. Rev.* **2005**, *105*, 1103−1169.

(6) Akkerman, H. B.; Blom, P. W. M.; de Leeuw, D. M.; de Boer, B. Towards Molecular Electronics with Large-Area Molecular Junctions. *Nature* **2006**, *441*, 69−72.

(7) Song, H.; Reed, M. A.; Lee, T. Single Molecule Electronic Devices. *Adv. Mater.* **2011**, *23*, 1583−1608.

(8) Wang, G.; Kim, T.-W.; Lee, T. Electrical Transport Characteristics through Molecular Layers. *J. Mater. Chem.* **2011**, *21*, 18117−18136.

(9) Park, H.; Park, J.; Lim, A. K. L.; Anderson, E. H.; Alivisatos, A. P.; McEuen, P. L. Nanomechanical Oscillations in a Single-C_{60} Transistor. *Nature* **2000**, *407*, 57−60.

(10) Green, J. E.; et al. A 160-Kilobit Molecular Electronic Memory Patterned at 10^{11} Bits Per Square Centimetre. *Nature* **2007**, *445*, 414−417.

(11) Kronemeijer, A. J.; Akkerman, H. B.; Kudernac, T.; van Wees, B. J.; Feringa, B. L.; Blom, P. W. M.; de Boer, B. Reversible Conductance Switching in Molecular Devices. *Adv. Mater.* **2008**, *20*, 1467−1473.

(12) Nijhuis, C. A.; Reus, W. F.; Whitesides, G. M. Molecular Rectification in Metal-Sam-Metal Oxide-Metal Junctions. *J. Am. Chem. Soc.* **2009**, *131*, 17814−17827.

(13) Quek, S. Y.; Kamenetska, M.; Steigerwald, M. L.; Choi, H. J.; Louie, S. G.; Hybertsen, M. S.; Neaton, J. B.; Venkataraman, L. Mechanically Controlled Binary Conductance Switching of a Single-Molecule Junction. *Nat. Nanotechnol.* **2009**, *4*, 230−234.

(14) Kornilovitch, P. E.; Bratkovsky, A. M.; Williams, R. S. Current Rectification by Molecules with Asymmetric Tunneling Barriers. *Phys. Rev. B: Condens. Matter Mater. Phys.* **2002**, *66*, 165436.

(15) Diez-Perez, I.; Hihath, J.; Lee, Y.; Yu, L.; Adamska, L.; Kozhushner, M. A.; Oleynik, I. I.; Tao, N. Rectification and Stability of a Single Molecular Diode with Controlled Orientation. *Nat. Chem.* **2009**, *1*, 635−641.

(16) Nijhuis, C. A.; Reus, W. F.; Siegel, A. C.; Whitesides, G. M. A Molecular Half-Wave Rectifier. *J. Am. Chem. Soc.* **2011**, *133*, 15397−15411.

(17) Loertscher, E.; Gotsmann, B.; Lee, Y.; Yu, L.; Rettner, C.; Riel, H. Transport Properties of a Single-Molecule Diode. *ACS Nano* **2012**, *6*, 4931−4939.

(18) Yoon, H. J.; Liao, K.-C.; Lockett, M. R.; Kwok, S. W.; Baghbanzadeh, M.; Whitesides, G. M. Rectification in Tunneling Junctions: 2,2′-Bipyridyl-Terminated n-Alkanethiolates. *J. Am. Chem. Soc.* **2014**, *136*, 17155−17162.

(19) Capozzi, B.; Xia, J.; Adak, O.; Dell, E. J.; Liu, Z.-F.; Taylor, J. C.; Neaton, J. B.; Campos, L. M.; Venkataraman, L. Single-Molecule Diodes with High Rectification Ratios through Environmental Control. *Nat. Nanotechnol.* **2015**, *10*, 522−527.

(20) Yuan, L.; Breuer, R.; Jiang, L.; Schmittel, M.; Nijhuis, C. A. A Molecular Diode with a Statistically Robust Rectification Ratio of Three Orders of Magnitude. *Nano Lett.* **2015**, *15*, 5506−5512.

(21) Jeong, H.; et al. Redox-Induced Asymmetric Electrical Characteristics of Ferrocene- Alkanethiolate Molecular Devices on Rigid and Flexible Substrates. *Adv. Funct. Mater.* **2014**, *24*, 2472−2480.

(22) Park, S.; Wang, G.; Cho, B.; Kim, Y.; Song, S.; Ji, Y.; Yoon, M.-H.; Lee, T. Flexible Molecular-Scale Electronic Devices. *Nat. Nanotechnol.* **2012**, *7*, 438−442.

(23) de Boer, B.; Frank, M. M.; Chabal, Y. J.; Jiang, W. R.; Garfunkel, E.; Bao, Z. Metallic Contact Formation for Molecular Electronics: Interactions between Vapor-Deposited Metals and Self-Assembled Monolayers of Conjugated Mono- and Dithiols. *Langmuir* **2004**, *20*, 1539−1542.

(24) Haick, H.; Cahen, D. Contacting Organic Molecules by Soft Methods: Towards Molecule-Based Electronic Devices. *Acc. Chem. Res.* **2008**, *41*, 359−366.

(25) Na, S.-I.; Wang, G.; Kim, S.-S.; Kim, T.-W.; Oh, S.-H.; Yu, B.-K.; Lee, T.; Kim, D.-Y. Evolution of Nanomorphology and Anisotropic Conductivity in Solvent-Modified PEDOT:PSS Films for Polymeric Anodes of Polymer Solar Cells. *J. Mater. Chem.* **2009**, *19*, 9045−9053.

(26) Wold, D. J.; Frisbie, C. D. Fabrication and Characterization of Metal-Molecule-Metal Junctions by Conducting Probe Atomic Force Microscopy. *J. Am. Chem. Soc.* **2001**, *123*, 5549−5556.

(27) Rampi, M. A.; Whitesides, G. M. A Versatile Experimental Approach for Understanding Electron Transport through Organic Materials. *Chem. Phys.* **2002**, *281*, 373−391.

(28) Kim, T.-W.; Wang, G.; Lee, H.; Lee, T. Statistical Analysis of Electronic Properties of Alkanethiols in Metal-Molecule-Metal Junctions. *Nanotechnology* **2007**, *18*, 315204.

(29) Jiang, L.; Yuan, L.; Cao, L.; Nijhuis, C. A. Controlling Leakage Currents: The Role of the Binding Group and Purity of the Precursors for Self-Assembled Monolayers in the Performance of Molecular Diodes. *J. Am. Chem. Soc.* **2014**, *136*, 1982−1991.

(30) Yuan, L.; Jiang, L.; Thompson, D.; Nijhuis, C. A. On the Remarkable Role of Surface Topography of the Bottom Electrodes in Blocking Leakage Currents in Molecular Diodes. *J. Am. Chem. Soc.* **2014**, *136*, 6554−6557.

(31) Choi, S. H.; Risko, C.; Delgado, M. C. R.; Kim, B.; Bredas, J.-L.; Frisbie, C. D. Transition from Tunneling to Hopping Transport in Long, Conjugated Oligo-imine Wires Connected to Metals. *J. Am. Chem. Soc.* **2010**, *132*, 4358−4368.

(32) Hines, T.; Diez-Perez, I.; Hihath, J.; Liu, H.; Wang, Z.-S.; Zhao, J.; Zhou, G.; Mullen, K.; Tao, N. Transition from Tunneling to Hopping in Single Molecular Junctions by Measuring Length and Temperature Dependence. *J. Am. Chem. Soc.* **2010**, *132*, 11658−11664.

(33) Poot, M.; Osorio, E.; O'Neill, K.; Thijssen, J. M.; Vanmaekelbergh, D.; van Walree, C. A.; Jenneskens, L. W.; van der Zant, S. J. Temperature Dependence of Three-Terminal Molecular Junctions with Sulfur End-Functionalized Tercyclohexylidenes. *Nano Lett.* **2006**, *6*, 1031−1035.

(34) Selzer, Y.; Cabassi, M. A.; Mayer, T. S.; Allara, D. L. Temperature Effects on Conduction through a Molecular Junction. *Nanotechnology* **2004**, *15*, S483−S488.

(35) Cuevas, J. C.; Scheer, E. *Molecular Electronics: An Introduction to Theory and Experiment*; World Scientific: Singapore, 2010.

(36) Cuniberti, G.; Fagas, G.; Richter, K. *Introducing Molecular Electronics*; Springer: New York, 2005.

(37) Castagnola, M.; Floris, B.; Illuminati, G.; Ortaggi, G. The Electron Donor Properties of Ferrocene. The Oxidation of Ferrocene by Carboxylic Acids. *J. Organomet. Chem.* **1973**, *60*, C17−C18.

(38) Tivanski, A. V.; Walker, G. C. Ferrocenylundecanethiol Self-Assembled Monolayer Charging Correlates with Negative Differential Resistance Measured by Conducting Probe Atomic Force Microscopy. *J. Am. Chem. Soc.* **2005**, *127*, 7647−7653.

(39) Ye, S.; Sato, Y.; Uosaki, K. Redox-Induced Orientation Change of a Self-Assembled Monolayer of 11-Ferrocenyl-1-Undecanethiol on a Gold Electrode Studied by in Situ FT-IRRAS. *Langmuir* **1997**, *13*, 3157−3161.

(40) Xiao, X.; Brune, D.; He, J.; Lindsay, S.; Gorman, C. B.; Tao, N. Redox-Gated Electron Transport in Electrically Wired Ferrocene Molecules. *Chem. Phys.* **2006**, *326*, 138−143.

(41) Slowinski, K.; Chamberlain, R. V.; Miller, C. J.; Majda, M. Through-Bond and Chain-to-Chain Coupling. Two Pathways in Electron Tunneling through Liquid Alkanethiol Monolayers on Mercury Electrodes. *J. Am. Chem. Soc.* **1997**, *119*, 11910−11919.

(42) Yamamoto, H.; Waldeck, D. H. Effect of Tilt-Angle on Electron Tunneling through Organic Monolayer Films. *J. Phys. Chem. B* **2002**, *106*, 7469−7473.

(43) Nerngchamnong, N.; Yuan, L.; Qi, D.-C.; Li, J.; Thompson, D.; Nijhuis, C. A. The Role of Van Der Waals Forces in the Performance of Molecular Diodes. *Nat. Nanotechnol.* **2013**, *8*, 113−118.

(44) Beebe, J. M.; Kim, B.; Gadzuk, J. W.; Frisbie, C. D.; Kushmerick, J. G. Transition from Direct Tunneling to Field Emission in Metal-Molecule-Metal Junctions. *Phys. Rev. Lett.* **2006**, *97*, 026801.

(45) Beebe, J. M.; Kim, B.; Frisbie, C. D.; Kushmerick, J. G. Measuring Relative Barrier Heights in Molecular Electronic Junctions with Transition Voltage Spectroscopy. *ACS Nano* **2008**, *2*, 827−832.

(46) Bennett, N.; Xu, G.; Esdaile, L. J.; Anderson, H. L.; Macdonald, J. E.; Elliott, M. Transition Voltage Spectroscopy of Porphyrin Molecular Wires. *Small* **2010**, *6*, 2604−2611.

(47) Huisman, E. H.; Guedon, C. M.; van Wees, B. J.; van der Molen, S. J. Interpretation of Transition Voltage Spectroscopy. *Nano Lett.* **2009**, *9*, 3909−3913.

(48) Markussen, T.; Chen, J.; Thygesen, K. S. Improving Transition Voltage Spectroscopy of Molecular Junctions. *Phys. Rev. B: Condens. Matter Mater. Phys.* **2011**, *83*, 155407.

(49) Wang, G.; Kim, Y.; Na, S.-I.; Kahng, Y. H.; Ku, J.; Park, S.; Jang, Y. H.; Kim, D.-Y.; Lee, T. Investigation of the Transition Voltage Spectra of Molecular Junctions Considering Frontier Molecular Orbitals and the Asymmetric Coupling Effect. *J. Phys. Chem. C* **2011**, *115*, 17979−17985.

(50) Baldea, I. Ambipolar Transition Voltage Spectroscopy: Analytical Results and Experimental Agreement. *Phys. Rev. B: Condens. Matter Mater. Phys.* **2012**, *85*, 035442.

(51) Wang, G.; Kim, T.-W.; Lee, H.; Lee, T. Influence of Metal-Molecule Contacts on Decay Coefficients and Specific Contact Resistances in Molecular Junctions. *Phys. Rev. B: Condens. Matter Mater. Phys.* **2007**, *76*, 205320.

(52) Guo, S.; Hihath, J.; Diez-Perez, I.; Tao, N. Measurement and Statistical Analysis of Single-Molecule Current-Voltage Characteristics, Transition Voltage Spectroscopy, and Tunneling Barrier Height. *J. Am. Chem. Soc.* **2011**, *133*, 19189−19197.

(53) Wang, G.; Na, S.-I.; Kim, T.-W.; Kim, Y.; Park, S.; Lee, T. Effect of PEDOT:PSS-Molecule Interface on the Charge Transport Characteristics of the Large-Area Molecular Electronic Junctions. *Org. Electron.* **2012**, *13*, 771−777.

(54) Tomfohr, J. K.; Sankey, O. F. Complex Band Structure, Decay Lengths, and Fermi Level Alignment in Simple Molecular Electronic Systems. *Phys. Rev. B: Condens. Matter Mater. Phys.* **2002**, *65*, 245105.

(55) Salomon, A.; Cahen, D.; Lindsay, S.; Tomfohr, J.; Engelkes, V. B.; Frisbie, C. D. Comparison of Electronic Transport Measurements on Organic Molecules. *Adv. Mater.* **2003**, *15*, 1881−1890.

(56) Dhungana, K. B.; Mandal, S.; Pati, R. Switching of Conductance in a Molecular Wire: Role of Junction Geometry, Interfacial Distance, and Conformational Change. *J. Phys. Chem. C* **2012**, *116*, 17268−17273.

(57) Song, H.; Lee, H.; Lee, T. Intermolecular Chain-to-Chain Tunneling in Metal-Alkanethiol-Metal Junctions. *J. Am. Chem. Soc.* **2007**, *129*, 3806−3807.

(58) Wang, G.; Kim, T.-W.; Jo, G.; Lee, T. Enhancement of Field Emission Transport by Molecular Tilt Configuration in Metal-Molecule-Metal Junctions. *J. Am. Chem. Soc.* **2009**, *131*, 5980−5985.

(59) Diez-Perez, I.; Hihath, J.; Hines, T.; Wang, Z.-S.; Zhou, G.; Muellen, K.; Tao, N. Controlling Single-Molecule Conductance through Lateral Coupling of π Orbitals. *Nat. Nanotechnol.* **2011**, *6*, 226−231.